Numer. Math. Theor. Meth. Appl.
doi: 10.4208/nmtma.OA-2022-0078

Vol. **16**, No. 1, pp. 204-229
February 2023

A Structure-Preserving JKO Scheme for the Size-Modified Poisson-Nernst-Planck-Cahn-Hilliard Equations

Jie Ding[1,*] and Xiang Ji[2]

[1] *School of Science, Jiangnan University, Wuxi, Jiangsu, 214122, China*
[2] *Department of Mathematics and Mathematical Center for Interdiscipline Research, Soochow University, 1 Shizi Street, Suzhou 215006, Jiangsu, China*

Received 9 May 2022; Accepted (in revised version) 19 August 2022

Abstract. In this paper, we propose a structure-preserving numerical scheme for the size-modified Poisson-Nernst-Planck-Cahn-Hilliard (SPNPCH) equations derived from the free energy including electrostatic energies, entropies, steric energies, and Cahn-Hilliard mixtures. Based on the Jordan-Kinderlehrer-Otto (JKO) framework and the Benamou-Brenier formula of quadratic Wasserstein distance, the SPNPCH equations are transformed into a constrained optimization problem. By exploiting the convexity of the objective function, we can prove the existence and uniqueness of the numerical solution to the optimization problem. Mass conservation and unconditional energy-dissipation are preserved automatically by this scheme. Furthermore, by making use of the singularity of the entropy term which keeps the concentration from approaching zero, we can ensure the positivity of concentration. To solve the optimization problem, we apply the quasi-Newton method, which can ensure the positivity of concentration in the iterative process. Numerical tests are performed to confirm the anticipated accuracy and the desired physical properties of the developed scheme. Finally, the proposed scheme can also be applied to study the influence of ionic sizes and gradient energy coefficients on ion distribution.

AMS subject classifications: 35K55, 35J05, 65M06, 65M12

Key words: Structure-preserving, size-modified Poisson-Nernst-Planck-Cahn-Hilliard equations, JKO framework, positivity.

1. Introduction

The classical Poisson-Nernst-Planck (cPNP) equation is a continuum mean-field model, which can describe the ionic transport in semiconductors, ion channels, and electrochemical devices. The cPNP equations include the Poisson's equation and the

*Corresponding author. *Email address:* jding@jiangnan.edu.cn (J. Ding)

Nernst-Planck (NP) equations. The Poisson's equation can determine the electrical potential induced by the ionic concentration. According to the Fick and Kohlrausch laws, the NP equations describe electro-diffusion and electrophoresis. Despite its usefulness in a variety of applications, the cPNP equations show unphysical crowding of ions near charged surfaces and incorrect dynamics of ion transport, due to the ignored steric effects of ions in its mean-field derivation. To incorporate the steric effects of ions in the PNP model, one technique is to include the interaction energy, which can be the density functional theory [12, 13, 36] or the Lennard-Jones potential [9, 14, 16, 23] for the hard-sphere repulsions. Another technique is to add the entropy of solvent molecules to the electrostatic free energy [17, 19, 21, 30, 35], which is known as the Borukhov model [2]. Employing the consideration of the entropy of solvent molecules in the free energy functional, Lu *et al.* [30] get a class of size-modified Poisson-Nernst-Planck (SMPNP) equations.

In this paper, in addition to incorporating the entropy of solvent molecules in the free energy functional, we also consider the concentration gradient energies utilized in the Ginzburg-Landau theory to describe phase separation [10, 11]. A conserved H^{-1} gradient flow of the Ginzburg-Landau functional gives rise to the Cahn-Hilliard equations [3]. Therefore, the free energy arising from electrostatic energies, entropies, steric energies, and Cahn-Hilliard mixtures leads to the following size-modified Poisson-Nernst-Planck-Cahn-Hilliard (SPNPCH) equations:

$$\begin{cases} \partial_t c^l = \gamma_l \nabla \cdot c^l \nabla \left[\log v_l c^l + q^l \psi - \dfrac{v_l}{v_0} \log \left(1 - \sum\limits_{k=1}^{M} v_k c^k \right) - \sigma^l \Delta c^l \right] \\ \qquad\qquad \text{in } \Omega, \quad l = 1, 2, \ldots, M, \\ -\kappa \Delta \psi = \sum\limits_{l=1}^{M} q^l c^l + \rho^f \quad \text{in } \Omega, \end{cases} \tag{1.1}$$

where c^l denotes the concentration of l-th ionic species, q^l denotes the valence of l-th ionic species, v_l denotes the volume of l-th ionic species, v_0 denotes the volume of the solvent molecule, σ^l denotes gradient energy coefficient of l-th ionic species, Ω denotes the charged system, ψ denotes the electrostatic potential, ρ^f denotes the fixed charge density, and κ and γ_l denote two nondimensionalized coefficients.

In the closed system, the PNP-type equations have three physical properties: total mass conservative, the positivity of ionic concentration, and energy dissipation. Much effort is devoted to developing the PNP-type scheme to preserve the above properties by using finite difference method, finite volume method, and finite element method. A finite element scheme for the PNP-type equations was developed in [31] to ensure the positivity of ionic concentration via a variable transformation. An arbitrary-order free energy satisfying a discontinuous Galerkin method for 1-D PNP equations was constructed in [28] to meet the energy dissipation law, in which the positivity of numerical solutions is enforced by an accuracy-preserving limiter. An implicit finite difference method for PNP equations to satisfy three physical properties was designed in [8, 15].

Shen and Xu [37] propose a set of numerical schemes for PNP equations that preserve unconditionally positivity, unique solvability, and energy dissipation. Based on the gradient-flow formulation, Wang *et al.* [24, 25, 34] propose a mass conservative, positivity-preserving, and energy stable finite difference scheme and establish an optimal rate convergence analysis. Based on the Slotboom variables [39], the NP equations are transformed into the form of heat equations. In [7,8,15,26,27,38] design a set of fully-discrete numerical schemes that can preserve the positivity of the numerical solutions. In this condition, unconditional energy dissipation can be proved with implicit electric potential.

Apart from the above-mentioned approaches, the JKO scheme [18,32] can preserve the mass conservation, positivity, and unconditional energy dissipation for the Fokker-Planck (FP) equation. The JKO scheme constructs a time-discrete, iterative variational scheme for the FP equation and the time step is governed by the Wasserstein distance on the probability measure. Following [20], the SPNPCH equations can also be interpreted as a Wasserstein gradient flow concerning the free energy $F(c)$ defined on $\mathbb{K}(\Omega)$ [20]

$$\mathbb{K}(\Omega)=\left\{c=(c^1,c^2,\cdots,c^M):c^l>0,\ \frac{1}{m(\Omega)}\int_\Omega c^l\,dV=S_l,\ l=1,2,\ldots,M\right\},$$

where $m(\Omega)$ is the Lebesgue measure of Ω, and S_l is the total mass of l-th ionic species with reference to the Lebesgue measure. Therefore, $\mathbb{K}(\Omega)\in L^1(\Omega;R_+)$. Given two measures $\rho_1,\rho_2\in\mathbb{K}(\Omega)$, the square Wasserstein distance W_2 is denoted by [1,33,40]

$$W_2^2(\rho_1,\rho_2):=\min_{\mu\in\Gamma(\rho_1,\rho_2)}\int\int_{\Omega\times\Omega}|\mathbf{x}-\mathbf{y}|^2\,d\mu(\mathbf{x},\mathbf{y})$$

with the set given by

$$\Gamma(\rho_1,\rho_2)=\big\{\mu\in\mathbb{K}(\Omega\times\Omega):\mu_1=\rho_1,\ \mu_2=\rho_2\big\},$$

where μ_1 and μ_2 denote the first and second marginal measure, respectively. Then, given the initial data $c_{in}=(c_{in}^1,c_{in}^2,\cdots,c_{in}^M)$ and a uniform time step $\Delta t>0$, the implicit JKO scheme of SPNPCH equations defines a sequence $\{c^n\}_{n\in\mathbb{N}}$ as

$$\begin{cases}c^0=c_{in},\\ c^{n+1}=\underset{c\in\mathbb{K}^M(\Omega)}{\arg\min}\left\{\sum\limits_{l=1}^{M}\dfrac{1}{2\gamma_l\Delta t}W_2^2(c^l,c^{l,n})+F(c)\right\}.\end{cases}\tag{1.2}$$

Here, $c^n=(c^{1,n},c^{2,n},\cdots,c^{M,n})$. Using this sequence, $c^{l,n}(\mathbf{x})$ can be expressed as numerical approximations of $c^l(t_n,\mathbf{x})$ with $t_n=n\Delta t$. The above scheme (1.2) can preserve mass conservative, the positivity, and energy dissipation automatically. However, computing $W_2^2(c^l,c^{l,n})$, which is an infinite-dimensional minimization problem, may result in the loss of several physical properties. Adapting Benamou-Brenier's dynamic formulation, [22,41] offer the reformulated JKO scheme which combines a Fisher information regularization term to maintain the positivity of numerical solutions and energy

dissipation automatically. Without an additional stabilization term, Cancès *et al.* [4] replace the Wasserstein distance with the weighted H^{-1} norm and takes advantage of the monotonicity of the involved operators to preserve the positivity.

Our goal in this work is to develop structure-preserving numerical methods for the SPNPCH equations. Based on the JKO scheme, we transform the SPNPCH equations into a constrained optimization problem. To avoid direct computing the quadratic Wasserstein distance W_2, we adapt the weighted H^{-1} norm to replace W_2 owing to [33, 40]. In this way, we can prove the discrete objective function is strictly convex. Subsequently, the existence and uniqueness of the minimizer can be proved. To preserve the positivity of the concentration, by referring to [5, 24, 25, 34], we use the singularity of the entropy to keep the concentration from approaching zero. Since the entropy includes the component of the steric effect, the nonlinear coupling of the SPNPCH equations becomes stronger than cPNP equations, which brings many difficulties in numerical computation. Thus, we adapt the quasi-Newton method to compute, which can ensure the positivity in the iterative process. Numerical tests can demonstrate that the discrete JKO-1 scheme has anticipated accuracy and structure-preserving properties. Finally, our scheme can be applied to explore the impact of ionic sizes and gradient energy coefficients on ionic distribution.

This paper is organized as follows. In Section 2, we derive the SPNPCH equations from the free energy consisting of the electrostatic energy, the entropy, the steric energy, and the Cahn-Hilliard mixtures. In Section 3, we propose the constraint JKO scheme combined with the weighted H^{-1} norm. In Section 4, we provide the fully-discrete JKO-1 scheme and demonstrate three physical properties of the JKO-1 scheme. In numerical computation, we use the quasi-Newton method to solve the optimization problem. In Section 5, numerical tests are provided. Finally, we conclude in Section 6.

2. Governing equations

We consider a charged system with fixed charges ρ^f and M mobile ionic species, occupying a bounded, convex domain Ω with a smooth boundary $\partial\Omega$. The boundary can be separated into two types: Dirichlet-type $\Gamma_{\rm D}$ and Neumann-type $\Gamma_{\rm N}$, with $\Gamma_{\rm D}\bigcap\Gamma_{\rm N}=\varnothing$ and $\Gamma_{\rm D}\bigcup\Gamma_{\rm N}=\partial\Omega$. The electrostatic potential ψ solves the boundary-value problem of the Poisson's equation as follows:

$$\begin{cases} -\nabla\cdot\varepsilon_0\varepsilon_r\nabla\psi=\rho & \text{in } \Omega,\\ \varepsilon_0\varepsilon_r\dfrac{\partial\psi}{\partial\mathbf{n}}=\sigma & \text{on } \Gamma_{\rm N},\\ \psi=\psi_{\rm D} & \text{on } \Gamma_{\rm D}, \end{cases} \tag{2.1}$$

where ε_0 is the vacuum permittivity, ε_r is the dielectric coefficient, σ is the surface charge, $\psi_{\rm D}$ is the given electrostatic potential, and ρ is the charge density given by

$$\rho=\sum_{l=1}^{M}z^lc^l+\rho^f.$$

Here, $c^l(\mathbf{x},t)$ is l-th ionic concentration, $z^l = q^l e$ with e being the elementary charge and q^l being the valence of l-th ionic species.

Denote by $c = (c^1, c^2, \cdots, c^M)$. We study the mean-field free energy functional

$$F[c] = F_{pot}[c] + F_{ent}[c] + F_{ste}[c] + F_{c-h}[c] + F_{cp}[c]. \tag{2.2}$$

Here, the electrostatic potential energy, ideal-gas entropy, steric interaction energy, Cahn-Hilliard mixture, and the chemical potential of the system are

$$\begin{aligned}
F_{pot}[c] &= \int_\Omega \frac{1}{2}\rho\psi \, dV + \frac{1}{2}\int_{\Gamma_N} \sigma\psi \, dS - \frac{1}{2}\int_{\Gamma_D} \varepsilon_0\varepsilon_r \frac{\partial\psi}{\partial\mathbf{n}}\psi_D \, dS,\\
F_{ent}[c] &= \int_\Omega \beta^{-1}\sum_{l=1}^M c^l \Big[\log\left(v_l c^l\right) - 1\Big] \, dV,\\
F_{ste}[c] &= \int_\Omega \beta^{-1} c^0 \Big[\log\left(v_0 c^0\right) - 1\Big] \, dV,\\
F_{c-h}[c] &= \int_\Omega \sum_{l=1}^M \frac{\sigma^l}{2}|\nabla c^l|^2 \, dV,\\
F_{cp}[c] &= -\int_\Omega \sum_{l=1}^M c^l \mu_l \, dV,
\end{aligned} \tag{2.3}$$

respectively. Here, β is the inverse thermal energy and μ_l is the chemical potential of l-th ionic species. In the steric effect energy, v_l is the volume of l-th ionic species, c^0 is the solvent concentration defined by

$$c^0(\mathbf{x},t) = v_0^{-1}\left(1 - \sum_{k=1}^M v_k c^k(\mathbf{x},t)\right)$$

and v_0 is the volume of solvent molecule.

To guarantee the total mass conservation and energy dissipation, we apply the homogeneous Neumann boundary condition

$$\begin{cases} c^l \dfrac{\partial \mu_l}{\partial \mathbf{n}}\Big|_{\partial\Omega} = 0, \\ \dfrac{\partial c^l}{\partial \mathbf{n}} = 0. \end{cases}$$

By taking the first variation of the free energy functional (2.2) and (2.3) with regard to c^l, we derive that the chemical potential of l-th ionic species satisfies [21, 29]

$$\mu_l = q^l\psi + \beta^{-1}\log\left(v_l c^l\right) - \beta^{-1}\frac{v_l}{v_0}\log\left(1 - \sum_{k=1}^M v_k c^k\right) - \sigma^l \Delta c^l.$$

As we used in [7], with the chemical potential, we obtain the size-modified Nernst-Planck equations

$$\partial_t c^l = \nabla \cdot D^l c^l \nabla \left[q^l \psi + \beta^{-1} \log v_l c^l - \beta^{-1} \frac{v_l}{v_0} \log \left(1 - \sum_{k=1}^{M} v_k c^k \right) - \sigma^l \Delta c^l \right], \tag{2.4}$$

where D^l is the diffusion coefficient of the l-th ionic species.

To get a nondimensional formulation, we introduce the following variables:

$$\tilde{\mathbf{x}} = \frac{\mathbf{x}}{L}, \quad \tilde{D}^l = \frac{D^l}{D_0}, \quad \tilde{t} = \frac{tD_0}{L\lambda_{\mathrm{D}}}, \quad \tilde{c}^l = \frac{c^l}{c_0}, \quad \tilde{\rho}^f = \frac{\rho^f}{ec_0},$$
$$\tilde{v}_l = v_l c_0, \quad \tilde{\sigma}^l = \frac{\sigma^l c_0 \beta}{L^2}, \quad \tilde{\psi} = \beta e \psi, \quad \tilde{\sigma} = \frac{\sigma}{Lec_0}, \quad \tilde{\psi}_D = \beta e \psi_D.$$

Here c_0 is a characteristic concentration, L is a macroscopic length scale, $\lambda_{\mathrm{D}} = \sqrt{\varepsilon_0 \varepsilon_r / (2\beta e^2 c_0)}$ is a characteristic screening length. With the above rescaling, dropping all the tildes, we obtain the nondimensionalized size-modified Poisson-Nernst-Planck-Cahn-Hilliard (SPNPCH) equations

$$\begin{cases} \partial_t c^l = \gamma_l \nabla \cdot \left[c^l \nabla \left(q^l \psi + \log v_l c^l - \dfrac{v_l}{v_0} \log \left(1 - \sum\limits_{k=1}^{M} v_k c^k \right) - \sigma^l \Delta c^l \right) \right], \\ -\kappa \Delta \psi = \sum\limits_{k=1}^{M} q^l c^l + \rho^f, \end{cases} \tag{2.5}$$

where $\gamma_l = \lambda_{\mathrm{D}} D^l / L$ and $\kappa = 2\lambda_{\mathrm{D}}^2 / L^2$. The nondimensionalized boundary conditions are

$$\begin{cases} \kappa \dfrac{\partial \psi}{\partial \mathbf{n}} = \sigma & \text{on } \Gamma_{\mathrm{N}}, \\ \psi = \psi_{\mathrm{D}} & \text{on } \Gamma_{\mathrm{D}}, \\ c^l \nabla \left[q^l \psi + \log v_l c^l - \dfrac{v_l}{v_0} \log \left(1 - \sum\limits_{k=1}^{M} v_k c^k \right) - \sigma^l \Delta c^l \right] \cdot \mathbf{n} = 0 & \text{on } \partial\Omega, \\ \nabla c^l \cdot \mathbf{n} = 0 & \text{on } \partial\Omega. \end{cases} \tag{2.6}$$

In this condition, the free energy becomes

$$\begin{aligned} F = \int_\Omega \left\{ \frac{1}{2} \rho \psi + \sum_{l=0}^{M} c^l \big(\log(v_l c^l) - 1 \big) + \sum_{l=1}^{M} \frac{\sigma^l}{2} |\nabla c^l|^2 \right\} dV \\ + \frac{1}{2} \int_{\Gamma_N} \sigma \psi \, dS - \frac{1}{2} \int_{\Gamma_D} \kappa \frac{\partial \psi}{\partial \mathbf{n}} \psi_D \, dS. \end{aligned} \tag{2.7}$$

Theorem 2.1. *The solution to the SPNPCH equations* (2.5) *and boundary conditions* (2.6) *satisfies*

$$\frac{dF}{dt} = -\sum_{l=1}^{M} \gamma_l \int_\Omega c^l |\nabla \mu_l|^2 \, dV + \int_{\Gamma_N} \frac{\partial \sigma}{\partial t} \psi \, dS - \int_{\Gamma_D} \kappa \frac{\partial \psi}{\partial \mathbf{n}} \frac{\partial \psi_D}{\partial t} \, dS, \quad t > 0.$$

Proof. Taking a derivative with respect to time, we have

$$\frac{dF}{dt} = \int_\Omega \sum_{l=1}^{M} \mu^l \frac{\partial c^l}{\partial t}\, dV + \frac{1}{2}\int_\Omega \left(\rho\frac{\partial \psi}{\partial t} - \frac{\partial \rho}{\partial t}\psi\right) dV + \frac{1}{2}\int_{\Gamma_N} \left(\frac{\partial \sigma}{\partial t}\psi + \sigma\frac{\partial \psi}{\partial t}\right) dS$$
$$- \frac{1}{2}\int_{\Gamma_D} \kappa\left[\frac{\partial}{\partial t}\left(\frac{\partial \psi}{\partial \mathbf{n}}\right)\psi_D + \frac{\partial \psi}{\partial \mathbf{n}}\frac{\partial \psi_D}{\partial t}\right] dS, \tag{2.8}$$

where we use $\frac{\partial c^l}{\partial \mathbf{n}} = 0$ in the first equality. By using the Poisson's equation, we have

$$\frac{1}{2}\int_\Omega \left(\rho\frac{\partial \psi}{\partial t} - \frac{\partial \rho}{\partial t}\psi\right) dV = \frac{1}{2}\int_{\Gamma_N} \left(\frac{\partial \sigma}{\partial t}\psi - \sigma\frac{\partial \psi}{\partial t}\right) dS$$
$$+ \frac{1}{2}\int_{\Gamma_D} \kappa\left[\frac{\partial}{\partial t}\left(\frac{\partial \psi}{\partial \mathbf{n}}\right)\psi_D - \frac{\partial \psi}{\partial \mathbf{n}}\frac{\partial \psi_D}{\partial t}\right] dS. \tag{2.9}$$

Substitution of (2.9) into (2.8) yields

$$\frac{dF}{dt} = -\sum_{l=1}^{M} \gamma_l \int_\Omega c^l |\nabla \mu_l|^2\, dV + \int_{\Gamma_N} \frac{\partial \sigma}{\partial t}\psi\, dS - \int_{\Gamma_D} \kappa\frac{\partial \psi}{\partial \mathbf{n}}\frac{\partial \psi_D}{\partial t}\, dS,$$

where the NP equation and $\frac{\partial \mu_l}{\partial \mathbf{n}}\big|_{\partial\Omega} = 0$ are applied. □

Remark 2.1. The boundary conditions imposed on ion concentration c^l and potential ψ are different from the above. On the one hand, to guarantee the mass conservative and energy dissipation, periodic boundary conditions can be applied on c^l and ψ. On the other hand, Robin boundary conditions can also be applied to potential ψ, i.e.,

$$\psi + a\varepsilon_r \frac{\partial \psi}{\partial \mathbf{n}}\bigg|_{\Gamma_R} = \psi_R.$$

Here, a is the thickness of the stern layer. The corresponding nondimensionalized free energy becomes

$$F = \int_\Omega \left\{\frac{1}{2}\rho\psi + \sum_{l=0}^{M} c^l\big(\log(v_l c^l) - 1\big) + \sum_{l=1}^{M} \frac{\sigma^l}{2}|\nabla c^l|^2\right\} dV$$
$$+ \frac{1}{2}\int_{\Gamma_N} \sigma\psi\, dS - \frac{1}{2}\int_{\Gamma_D} \kappa\frac{\partial \psi}{\partial \mathbf{n}}\psi_D\, dS + \frac{\kappa}{2a}\int_{\Gamma_R} \psi_R\psi\, dS.$$

In this condition, the time evolution of free energy is

$$\frac{dF}{dt} = -\sum_{l=1}^{M} \gamma_l \int_\Omega c^l |\nabla \mu_l|^2\, dV + \int_{\Gamma_N} \frac{\partial \sigma}{\partial t}\psi\, dS - \int_{\Gamma_D} \kappa\frac{\partial \psi}{\partial \mathbf{n}}\frac{\partial \psi_D}{\partial t}\, dS + \frac{\kappa}{a}\int_{\Gamma_R} \frac{\partial \psi_R}{\partial t}\psi\, dS.$$

Remark 2.2. Providing the boundary data σ, ψ_D and ψ_R are independent of time, we have

$$\frac{dF}{dt} = -\sum_{l=1}^{M} \gamma_l \int_\Omega c^l |\nabla \mu_l|^2\, dV \le 0.$$

3. The JKO semi-discrete scheme

In this section, we introduce the semi-discrete constrained JKO scheme in time. To approximate the quadratic Wasserstein distance (1.2), we use the weighted H^{-1} norm in [33, 40]

$$\|c^l - c^{l,n}\|_{H^{-1}_{c^{l,n}}} = W_2(c^l, c^{l,n}) + o\big(W_2(c^l, c^{l,n})\big), \quad c^l, c^{l,n} \in \mathbb{K}(\Omega). \tag{3.1}$$

In the weighted H^{-1} norm, we denote that

$$\|c^l - c^{l,n}\|_{H^{-1}_{c^{l,n}}} = \left\{ \sup_{\phi} \int_\Omega (c^l - c^{l,n})\phi \, dV \,\middle|\, \|\phi\|_{H^1_{c^{l,n}}} \le 1 \right\}, \quad \|\phi\|^2_{H^1_{c^{l,n}}} = \int_\Omega c^{l,n} |\nabla \phi|^2 \, dV.$$

Therefore,

$$\left\| \frac{c^l - c^{l,n}}{\gamma_l \Delta t} \right\|^2_{H^{-1}_{c^{l,n}}} = \|\mu_l\|^2_{H_{c^{l,n}}}.$$

Thus, μ_l is the solution to

$$\begin{cases} c^l - c^{l,n} - \gamma_l \Delta t \nabla \cdot (c^{l,n} \nabla \mu_l) = 0 & \text{in } \Omega, \quad l = 1, 2, \dots, M, \\ \nabla \mu_l \cdot \mathbf{n} = 0 & \text{on } \partial\Omega. \end{cases}$$

Replacing the quadratic Wasserstein distance in (1.2) with the weighted H^{-1} norm (3.1), the implicit JKO scheme of SPNPCH equations writes

$$\begin{cases} c^0 = c_{in}, \\ c^{n+1} = \underset{c \in \mathbb{K}^M(\Omega)}{\arg\min} \left\{ \sum\limits_{l=1}^{M} \dfrac{1}{2\gamma_l \Delta t} \|c^l - c^{l,n}\|^2_{H^{-1}_{c^{l,n}}} + F(c) \right\}. \end{cases} \tag{3.2}$$

Combining the boundary conditions (2.6), the above scheme (3.2) can be formulated as a constrained optimization problem and rewritten as

$$\begin{cases} c^0 = c_{in}, \\ c^{n+1} = \underset{c \in \mathbb{K}^M(\Omega)}{\arg\min} \left\{ \sum\limits_{l=1}^{M} \dfrac{1}{2\gamma_l \Delta t} \|c^l - c^{l,n}\|^2_{H^{-1}_{c^{l,n}}} + F(c) \right\} = \underset{c \in \mathbb{K}^M(\Omega)}{\arg\min}\, E^n(c), \\ \text{subject to:} \begin{cases} \left[q^l \psi + \log v_l c^l - \dfrac{v_l}{v_0} \log \left(1 - \sum\limits_{k=1}^{M} v_k c^k \right) - \sigma^l \Delta c^l \right] \cdot \mathbf{n} = 0, \\ \qquad\qquad l = 1, 2, \dots, M \quad \text{on } \partial\Omega, \\ -\kappa \Delta \psi = \sum\limits_{l=1}^{M} q^l c^l + \rho_f \qquad \text{in } \Omega, \\ \kappa \dfrac{\partial \psi}{\partial \mathbf{n}} = \sigma \qquad \text{on } \Gamma_N, \\ \psi = \psi_D \qquad \text{on } \Gamma_D. \end{cases} \end{cases} \tag{3.3}$$

Theorem 3.1. *The semi-discrete JKO scheme* (3.3) *obeys the energy dissipation law*

$$F(c^{n+1})+\sum_{l=1}^{M}\frac{1}{2\gamma_l\Delta t}\|c^{l,n+1}-c^{l,n}\|^2_{H^{-1}_{c^{l,n}}}\leq F(c^n)\quad \textit{for}\quad t>0.$$

This result is obvious, we skip the proof.

4. The fully-discrete scheme

4.1. Notations

For simplicity, we consider a 2D rectangular computational domain $\Omega=[a,b]^2$ with the Dirichlet-type boundary

$$\Gamma_D=\big\{(x,y):x=a\ \text{ or }\ b,\ a\leq y\leq b\big\}$$

and Neumann-type boundary

$$\Gamma_N=\big\{(x,y):y=a\ \text{ or }\ b,\ a\leq x\leq b\big\}.$$

The computational domain is covered by the uniform grid points

$$\{x_i,y_j\}=\left\{a+\left(i-\frac{1}{2}\right)h,a+\left(j-\frac{1}{2}\right)h\right\}\quad \text{for}\quad i,j=1,2,\ldots,N,$$

where $N=(b-a)/h$ is the number of grid points along each dimension and h is the step size of spatial mesh.

Introduce the following two different difference operators in x-direction:

$$D_xf_{i+\frac{1}{2},j}:=\frac{1}{h}\left(f_{i+1,j}-f_{i,j}\right),\quad d_xf_{i,j}:=\frac{1}{h}\left(f_{i+\frac{1}{2},j}-f_{i-\frac{1}{2},j}\right).$$

The difference operators D_y and d_y in y-direction can be defined similarly. The discrete gradient and discrete divergence are given by

$$\nabla_hf_{i,j}=\left(D_xf_{i+\frac{1}{2},j},D_yf_{i,j+\frac{1}{2}}\right),\quad \nabla_h\cdot\vec{f}_{i,j}=d_xf^x_{i,j}+d_yf^y_{i,j}.$$

Therefore, the 2D standard discrete Laplacian becomes

$$\Delta_hf_{i,j}:=\nabla_h\cdot(\nabla_hf)_{i,j}=d_x(D_xf)_{i,j}+d_y(D_yf)_{i,j}.$$

In addition, define the uniform grids

$$C:=\left\{p_i\,\middle|\,p_i=a+\left(i-\frac{1}{2}\right)h,\ i=1,2,\ldots,N\right\},$$

we introduce the following grid inner products on the domain Ω: for any grid function $f, g : C \times C \to \mathbb{R}$,

$$\langle f, g\rangle := h^2 \sum_{i,j=1}^{N} f_{i,j}\, g_{i,j}.$$

On the boundary Γ_D and Γ_N, the inner products become

$$\begin{aligned} \langle V, D_x f\rangle_D &:= h \sum_{j=1}^{N} \left(V_{N+\frac{1}{2},j} D_x f_{N+\frac{1}{2},j} - V_{\frac{1}{2},j} D_x f_{\frac{1}{2},j} \right), \\ \langle \sigma, f\rangle_N &:= h \sum_{i=1}^{N} \left(\sigma_{i,\frac{1}{2}} f_{i,\frac{1}{2}} + \sigma_{i,N+\frac{1}{2}} f_{i,N+\frac{1}{2}} \right), \end{aligned} \tag{4.1}$$

where σ represents the given surface charge and V represents the given applied voltage. The average on the half-grid points is discretized as

$$f_{i,j+\frac{1}{2}} = \frac{1}{2}(f_{i,j} + f_{i,j+1}). \tag{4.2}$$

Subsequently, we can define the following norms:

$$\|f\|_2^2 := \langle f, f\rangle, \quad \|f\|_\infty := \max_{1\le i,j\le N} |f_{i,j}|.$$

To define the discrete weighted H^1 norm and weighted H^{-1} norm, we introduce the following 2-D discrete homogeneous Neumann function space:

$$\begin{aligned} \mathcal{N}_1 &= \left\{ \nu \,\middle|\, \nu_{kN,j} = \nu_{kN+1,j},\ \nu_{i,kN} = \nu_{i,kN+1} \ \text{ for } \ k = 0, 1 \right\}, \\ \mathcal{N}_2 &= \left\{ \nu \,\middle|\, \sum_{i,j=1}^{N} \nu_{i,j} = 0,\ \nu_{kN,j} = \nu_{kN+1,j},\ \nu_{i,kN} = \nu_{i,kN+1} \ \text{ for } \ k = 0, 1 \right\}. \end{aligned}$$

For $\nu^1, \nu^2 \in \mathcal{N}_1$, the inner product on the half grids is defined by

$$[\nu^1, \nu^2]_x = h^2 \sum_{i,j=1}^{N} \nu^1_{i+\frac{1}{2},j} \nu^2_{i+\frac{1}{2},j}, \quad [\nu^1, \nu^2]_y = h^2 \sum_{i,j=1}^{N} \nu^1_{i,j+\frac{1}{2}} \nu^2_{i,j+\frac{1}{2}}.$$

Therefore, for $\vec{f} = (f_x, f_y)$, the inner product is

$$[\vec{f}, \vec{f}] := [f^x, f^x]_x + [f^y, f^y]_y.$$

Subsequently, the gradient norms are defined by

$$\|\nabla_h f\|_2^2 = [\nabla_h f, \nabla_h f].$$

For $g \in \mathcal{N}_2$, there exists a unique solution $\mu \in \mathcal{N}_2$ to

$$\mathcal{L}_f \mu := -\nabla_h \cdot (f \nabla_h \mu) = g, \tag{4.3}$$

where $f : C \times C \to \mathbb{R}$ is bounded below. If $f = 1$, we write $\mathcal{L}_1 \mu := \mathcal{L}\mu$ for simplicity. For $g_1, g_2 \in \mathcal{N}_2$, we define the inner product

$$\langle g_1, g_2 \rangle_{\mathcal{L}_f^{-1}} := [f \nabla_h \mu_1, \nabla_h \mu_2],$$

where

$$\mathcal{L}_f \mu_l = g_l \quad \text{for} \quad l = 1, 2.$$

Using this definition, the discrete weighted H^{-1} norm of $\|\mu\|_{H_f^1}$ is given by

$$\|g\|^2_{\mathcal{L}_f^{-1}} = \langle g, g \rangle_{\mathcal{L}_f^{-1}} = [f \nabla_h \mu, \nabla_h \mu],$$

where we use the equality (4.3). By using the summation by parts, we obtain

$$\|g\|^2_{\mathcal{L}_f^{-1}} = \langle \mathcal{L}_f^{-1} g, g \rangle = \langle g, \mathcal{L}_f^{-1} g \rangle.$$

4.2. The discrete Poisson's equation

Given $c_{i,j}^l$, the Poisson's equation is discretized by central differencing method

$$-\kappa \Delta_h \psi_{i,j} = \sum_{l=1}^{M} q^l c_{i,j}^l + \rho_{i,j}^f, \quad i, j = 1, \ldots, N. \tag{4.4}$$

The boundary conditions are discretized by

$$\begin{aligned}
&\frac{\psi_{0,j} + \psi_{1,j}}{2} = \psi_D(t_n, a, y_j), \\
&\frac{\psi_{N+1,j} + \psi_{N,j}}{2} = \psi_D(b, y_j) \quad \text{for} \quad j = 1, \ldots, N \quad \text{on } \Gamma_D, \\
&-\kappa D_y \psi_{i,0} = \sigma(x_i, a), \\
&\kappa D_y \psi_{i,N} = \sigma(x_i, b) \qquad\quad \text{for} \quad i = 1, \ldots, N \quad \text{on } \Gamma_N.
\end{aligned} \tag{4.5}$$

The boundary data ψ_D and σ have been extended to the entire computational domain. In numerical computation, the ghost points outside Ω are eliminated by the Poisson's scheme (4.4) and boundary discretization (4.5). Denote the discrete Poisson's equation (4.4) and the boundary discretization (4.5) satisfy

$$M_h\big(\psi, c^1, c^2, \cdots, c^M\big) = 0. \tag{4.6}$$

Let $\boldsymbol{\psi}$, $\boldsymbol{c}^l$, and $\boldsymbol{\rho}^f$ denote vectors with components being $\psi_{i,j}$, $c_{i,j}^l$, and $\rho_{i,j}^f$, respectively. The coupled difference equations can be written in a matrix form

$$\mathcal{P}_\kappa \boldsymbol{\psi} = \sum_{l=1}^{M} q^l \boldsymbol{c}^l + \boldsymbol{\rho}^f + \boldsymbol{b}. \tag{4.7}$$

Here $\mathcal{P}_\kappa$ is the coefficient matrix of negative Laplacian operator associated with κ and the boundary conditions (4.5), and the column vector $\boldsymbol{b}$ results from the boundary conditions (4.5).

4.3. First-order fully-discrete JKO scheme

The fully discrete objective function in (3.3) is given by

$$E_h^n(c) = \sum_{l=1}^{M} \frac{1}{2\gamma_l \Delta t} \|c^l - c^{l,n}\|^2_{\mathcal{L}^{-1}_{c^{l,n}}} + F_h(c), \tag{4.8}$$

where the free energy (2.7) is

$$\begin{aligned} F_h(c) = &\sum_{l=1}^{M} \left[\langle c^l, \log v_l c^l - 1 \rangle + \frac{1}{2} \langle q^l c^l + \rho^f, \psi \rangle + \frac{\sigma^l}{2} \left\| \nabla_h c^l \right\|_2^2 \right] \\ &+ \frac{1}{v_0} \left\langle 1 - \sum_{l=1}^{M} v_l c^l, \log \left(1 - \sum_{l=1}^{M} v_l c^l \right) - 1 \right\rangle \\ &+ \frac{1}{2} \langle \sigma, \psi_N \rangle - \frac{1}{2} \langle \psi_D, \kappa D_x \psi \rangle_D, \end{aligned} \tag{4.9}$$

which is a second-order accurate approximation of E^n (3.2) in space. The boundary inner product in (4.9) is discretized by the average mean (4.2) and discretized boundary data (4.5). Then, we arrive that the fully-discrete JKO scheme

$$\begin{cases} c^0 = c_{in}, \\ c^{n+1} = \underset{c \in \mathbb{K}_h^M}{\arg\min}\ E_h^n(c), \\ \text{s.t. } M_h\big(\psi, c^1, c^2, \cdots, c^M\big) = 0, \end{cases} \tag{4.10}$$

where

$$\mathbb{K}_h = \left\{ c \,\middle|\, c_{i,j}^l > 0,\ \frac{h^2}{|\Omega|} \sum_{i,j=1}^{N} c_{i,j}^l = S_l \ \text{ for } \ l = 1, 2, \ldots, M,\ i, j = 1, \ldots, N \right\}.$$

We refer to the above scheme (4.10) as the "JKO-1 scheme".

Using the technique in [5, 6], we present the following lemma without giving its proof.

Lemma 4.1. *Assume $\nu \in \mathcal{N}_2$, $\|\nu\|_\infty \le C_1$, and $\phi \ge C_2 > 0$, we get the following estimate:*

$$\left\| \mathcal{L}_\phi^{-1} \nu \right\|_\infty \le \tilde{C}_1 C_2^{-1} h^{-\frac{1}{2}},$$

where $\tilde{C}_1$ depends on Ω and C_1.

This lemma can help to prove the positivity of ionic concentration.

Theorem 4.1. *Assume that* $\|\mathcal{P}_\kappa^{-1}\|_\infty \le \hat{C}_1$, $\|\boldsymbol{\rho}^f\|_\infty \le \hat{C}_2$ *and* $\|\boldsymbol{b}\|_\infty \le \hat{C}_3$. *Define*

$$C_m^{l,n} := \min_{1\le i,j\le N} c_{i,j}^{l,n}$$

and $C_m^{l,n} > 0$. *Since* F_h (4.9) *is strictly convex, the following physical properties are satisfied:*

i) There exists a unique minimizer for the JKO-1 scheme (4.10).

ii) The charge density is positive, i.e.,

$$c_{i,j}^{l,n+1} > 0 \quad \textit{for} \quad i,j = 1,2,\dots,N.$$

iii) The mass is conserved

$$\sum_{i,j=1}^{N} c_{i,j}^{l,n+1} = \sum_{i,j=1}^{N} c_{i,j}^{l,n}.$$

iv) The discrete free energy (4.9) *decays*

$$F_h(c^{n+1}) + \sum_{l=1}^{M} \frac{1}{2\gamma_l \Delta t} \|c^{l,n+1} - c^{l,n}\|^2_{\mathcal{L}^{-1}_{c^{l,n}}} \le F_h(c^n) \quad \textit{for} \quad t > 0.$$

Proof. i) Consider the closed set $\mathbb{K}_{h,\delta} \subset \mathbb{K}_h$

$$\mathbb{K}_{h,\delta} := \left\{ c \,\middle|\, \delta \le c_{i,j}^l \le \xi_l - \delta,\ \frac{h^2}{|\Omega|} \sum_{i,j=1}^{N} c_{i,j}^l = S_l \ \text{ for } \ l = 1,2,\dots,M,\ i,j = 1,\dots,N \right\},$$

where $\xi_l = S_l|\Omega|/h^2$ and $\delta \in (0, \xi_l/2)$. Obviously, $\mathbb{K}_{h,\delta}$ is a bounded convex compact subset of $\mathbb{K}_h$. We prove that the objective function E_h^n of (4.8) is strictly convex in the Appendix A. Subsequently, there exists a unique minimizer in $\mathbb{K}_{h,\delta}^M$ for the JKO-1 scheme (4.10).

ii) According to the (i), there exists a unique minimizer of E_h^n over the domain $\mathbb{K}_{h,\delta}^M$. Suppose that the minimizer of E_h^n occurs at the boundary of $\mathbb{K}_{h,\delta}^M$ and the minimizer is $c^* = (c^{1*}, c^{2*}, \cdots, c^{M*})$. Assume there exists one grid point $\vec{\alpha}_0 = (i_0, j_0)$ and l_0 such that $c_{\vec{\alpha}_0}^{l_0 *} = \delta$. Similarly, we assume that the maximum of $c^{l_0 *}$ is at grid point $\vec{\alpha}_1 = (i_1, j_1)$. It is clear that the maximum value $c_{\vec{\alpha}_1}^{l_0 *}$ is larger than the mean value S_{l_0} and the minimum value $c_{\vec{\alpha}_0}^{l_0 *}$ is less than S_{l_0}, i.e.,

$$c_{\vec{\alpha}_1}^{l_0 *} \ge S_{l_0}, \quad c_{\vec{\alpha}_0}^{l_0 *} \le S_{l_0}.$$

Consider the following directional derivative:

$$\lim_{t\to 0^+}\frac{1}{t}\big(E_h^n(c^*+td)-E_h^n(c^*)\big)=\frac{1}{\gamma_{l_0}\Delta t}\big\langle\mathcal{L}^{-1}_{c^{l_0,n}}(c^{l_0,*}-c^{l_0,n}),d_{l_0}\big\rangle$$
$$+\left\langle q^{l_0}\psi(c^*)+\log v_{l_0}c^{l_0*}-\frac{v_{l_0}}{v_0}\log\left(1-\sum_{k=1}^{M}v_kc^{k*}\right)+\sigma^{l_0}\mathcal{L}c^{l_0*},d_{l_0}\right\rangle,$$

where t is sufficiently small and $d=(0,\cdots,0,d_{l_0},0,\cdots,0)$. Next, we choose the direction

$$d_{l_0}=\delta_{i,i_0}\delta_{j,j_0}-\delta_{i,i_1}\delta_{j,j_1},$$

where $\delta_{l,k}$ is the Kronecker delta function. As a result, the directional derivative becomes

$$\begin{aligned}&\frac{1}{h^2}\lim_{t\to 0^+}\frac{1}{t}\big(E_h^n(c^*+td)-E_h^n(c^*)\big)\\&=\frac{1}{\gamma_l\Delta t}\mathcal{L}^{-1}_{c^{l_0,n}}(c^{l_0*}-c^{l_0,n})_{\vec{\alpha}_0}-\frac{1}{\gamma_l\Delta t}\mathcal{L}^{-1}_{c^{l_0,n}}(c^{l_0*}-c^{l_0,n})_{\vec{\alpha}_1}\\&\quad+\left(q^{l_0}\psi(c^*)+\log v_{l_0}c^{l_0*}-\frac{v_{l_0}}{v_0}\log\left(1-\sum_{k=1}^{M}v_kc^{k*}\right)+\sigma^{l_0}\mathcal{L}c^{l_0*}\right)_{\vec{\alpha}_0}\\&\quad-\left(q^{l_0}\psi(c^*)+\log v_{l_0}c^{l_0*}-\frac{v_{l_0}}{v_0}\log\left(1-\sum_{k=1}^{M}v_kc^{k*}\right)+\sigma^{l_0}\mathcal{L}c^{l_0*}\right)_{\vec{\alpha}_1}.\end{aligned}\tag{4.11}$$

Since $c^{l_0*}_{\vec{\alpha}_0}=\delta$ and $c^{l_0*}_{\vec{\alpha}_1}\geq S_{l_0}$, we have

$$\log\big(v_{l_0}c^{l_0*}\big)_{\vec{\alpha}_0}-\log\big(v_{l_0}c^{l_0*}\big)_{\vec{\alpha}_1}\leq\log\delta-\log S_{l_0}.\tag{4.12}$$

By using the matrix form of Poisson' equation (4.7)

$$\mathcal{P}_\kappa\boldsymbol{\psi}^*=\sum_{k=1}^{M}q^k\boldsymbol{c}^{k*}+\boldsymbol{\rho}_f+\boldsymbol{b}\tag{4.13}$$

and

$$\big\|\mathcal{P}_\kappa^{-1}\big\|_\infty\leq\hat{C}_1,\quad\|\boldsymbol{c}^{k*}\|_\infty\leq\xi_l-\delta,\quad\|\boldsymbol{\rho}_f\|_\infty\leq\hat{C}_2,\quad\|\boldsymbol{b}\|_\infty\leq\hat{C}_3,$$

we obtain the following estimate:

$$\begin{aligned}&q^{l_0}\big[\psi(c^*)_{\vec{\alpha}_0}-\psi(c^*)_{\vec{\alpha}_1}\big]\leq 2|q^{l_0}|\|\boldsymbol{\psi}(\boldsymbol{c}^*)\|_\infty\\&\leq 2|q^{l_0}|\|\mathcal{P}_\kappa^{-1}\|_\infty\left(\sum_{k=1}^{M}|q^k|\|\boldsymbol{c}^{k*}\|_\infty+\|\boldsymbol{\rho}_f\|_\infty+\|\boldsymbol{b}\|_\infty\right)\\&\leq 2|q^{l_0}|\hat{C}_1\left(\sum_{k=1}^{M}|q^k|\xi_k+\hat{C}_2+\hat{C}_3\right):=C_0^*.\end{aligned}\tag{4.14}$$

Resulting from $0 < 1 - \sum_{k=1}^{M} v_k c^{k*} < 1$, we get

$$\frac{v_{l_0}}{v_0} \log \left(1 - \sum_{k=1}^{M} v_k c^{k*} \right) < 0. \tag{4.15}$$

Subsequently, we have the following result:

$$\begin{aligned} &\frac{v_{l_0}}{v_0} \log \left(1 - \sum_{k=1}^{M} v_k c^{k*} \right)_{\vec{\alpha}_1} - \frac{v_{l_0}}{v_0} \log \left(1 - \sum_{k=1}^{M} v_k c^{k*} \right)_{\vec{\alpha}_0} \\ \leq &-\frac{v_{l_0}}{v_0} \log \left(1 - \sum_{k=1}^{M} v_k \xi_k \right). \end{aligned} \tag{4.16}$$

Since c^{l_0*} achieves the minimum value at $\vec{\alpha}_0$ and the maximum value at $\vec{\alpha}_1$, we have

$$\sigma^{l_0} \mathcal{L} c^{l_0*}_{\vec{\alpha}_0} \leq 0, \quad \sigma^{l_0} \mathcal{L} c^{l_0*}_{\vec{\alpha}_1} \geq 0. \tag{4.17}$$

Therefore, we obtain

$$\sigma^{l_0} \mathcal{L} c^{l_0*}_{\vec{\alpha}_0} - \sigma^{l_0} \mathcal{L} c^{l_0*}_{\vec{\alpha}_1} \leq 0. \tag{4.18}$$

Resulting from $c^{l_0,n}_{i,j} \geq C^{l_0,n}_m$ and

$$\| c^{l_0*} - c^{l_0,n} \|_\infty \leq \xi_{l_0} - C^{l_0,n}_m,$$

we get

$$\mathcal{L}^{-1}_{c^{l_0,n}} (c^{l_0*} - c^{l_0,n})_{\vec{\alpha}_0} - \mathcal{L}^{-1}_{c^{l_0,n}} (c^{l_0*} - c^{l_0,n})_{\vec{\alpha}_1} \leq 2C^*_1, \tag{4.19}$$

where the Lemma 4.1 is applied and C^*_1 depends on $C^{l_0,n}_m$, h, Ω, and ξ_{l_0}.

Substituting (4.12)-(4.19) into (4.11) yields

$$\begin{aligned} &\frac{1}{h^2} \lim_{t \to 0^+} \frac{1}{t} \big(E^n_h(c^* + td) - E^n_h(c^*) \big) \\ \leq &\, 2(\gamma_{l_0} \Delta t)^{-1} C^*_1 + \log \delta - \log S_{l_0} + C^*_0 - \frac{v_{l_0}}{v_0} \log \left(1 - \sum_{k=1}^{M} v_k \xi_k \right). \end{aligned} \tag{4.20}$$

For any fixed Δt and h, we choose δ sufficiently small so that

$$2(\gamma_{l_0} \Delta t)^{-1} C^*_1 + \log \delta - \log S_{l_0} + C^*_0 - \frac{v_{l_0}}{v_0} \log \left(1 - \sum_{k=1}^{M} v_k \xi_k \right) < 0. \tag{4.21}$$

Therefore,

$$\lim_{t \to 0^+} \frac{1}{t} \big(E^n_h(c^* + td) - E^n_h(c^*) \big) < 0. \tag{4.22}$$

This is contradictory to the assumption that c^* is the minimizer of E^n_h.

Similarly, we can prove that the maximum value of E_h^n can not occur at the upper boundary $\mathbb{K}_{h,\delta}^M$. If this occurs, there must have some points c^* tending to zero. This contradicts the previous conclusion. Therefore, the global minimum of E_h^n could only possibly occur at an interior point. Since E_h^n is a smooth function, there must exist a solution $c^* \in \mathring{\mathbb{K}}_{h,\delta}^M \subset \mathring{\mathbb{K}}_h^M$, so that

$$\lim_{t\to 0^+} \frac{1}{t}\big(E_h^n(c^* + td) - E_h^n(c^*)\big) = 0. \tag{4.23}$$

In summary, there exists a unique positive numerical solution to the discrete JKO-1 scheme.

iii) Denote that c^{n+1} is the minimizer of the JKO-1 scheme (4.10). Therefore, c^{n+1} satisfies the Euler-Lagrange equations of the discrete JKO-1 scheme

$$\frac{c_{i,j}^{l,n+1} - c_{i,j}^{l,n}}{\gamma_l \Delta t} + \mathcal{L}_{c_{i,j}^{l,n}} \mu_{l,i,j}^{n+1} = 0 \quad \text{for} \quad l = 1, 2, \ldots, M, \;\; i, j = 1, 2, \ldots, N,$$

$$\mu_{l,i,j}^{n+1} = q^l \psi(c_{i,j}^{l,n+1}) + \log v_l c_{i,j}^{l,n+1} - \frac{v_l}{v_0} \log\left(1 - \sum_{k=1}^{M} v_k c_{i,j}^{k,n+1}\right) + \sigma^l \mathcal{L} c_{i,j}^{l,n+1}.$$

The above equation is summed over i, j and applied the discrete summation by the parts, we can get

$$\sum_{i,j=1}^{N} c_{i,j}^{l,n+1} = \sum_{i,j=1}^{N} c_{i,j}^{l,n} \quad \text{for} \quad l = 1, 2, \ldots, M,$$

where $\mu_l^{n+1} \in \mathcal{N}_1$.

iv) Denote that c^{n+1} is the minimizer of the JKO-1 scheme (4.10). Thus, we can get

$$E_h^n(c^{n+1}) \le E_h^n(c^n).$$

This implies

$$F_h(c^{n+1}) + \sum_{l=1}^{M} \frac{1}{2\gamma_l \Delta t} \|c^{l,n+1} - c^{l,n}\|_{\mathcal{L}_{c^{l,n}}^{-1}}^2 \le F_h(c^n) \quad \text{for} \quad t > 0.$$

As a result, the free energy decays. □

4.4. The Quasi-Newton's method

Denote the minimizer of E_h^n as c^{n+1}. The Euler-Lagrange equation of the JKO-1 scheme (4.10) in a vector form is

$$\frac{1}{\gamma_l \Delta t} \mathcal{A}_{\boldsymbol{c}^{l,n}}^{-1} (\boldsymbol{c}^{l,n+1} - \boldsymbol{c}^{l,n}) + \boldsymbol{\mu}_l^{n+1} = 0, \tag{4.24a}$$

$$\boldsymbol{\mu}_l^{n+1} = q^l\boldsymbol{\psi}^{n+1} + \log v_l\boldsymbol{c}^{l,n+1} - \frac{v_l}{v_0}\log\left(1-\sum_{r=1}^{M} v_r\boldsymbol{c}^{r,n+1}\right) + \sigma^l\mathcal{A}\boldsymbol{c}^{l,n+1}, \quad l=1,2,\ldots,M, \tag{4.24b}$$

where $\mathcal{A}_{\boldsymbol{c}^{l,n}}$, $\mathcal{A}$ is the discrete coefficient matrix of operator $\mathcal{L}_{\boldsymbol{c}^{l,n}}$ and $\mathcal{L}$, respectively. Let $\boldsymbol{u}^l = \log \boldsymbol{c}^l$, $\boldsymbol{u} = (\boldsymbol{u}^1, \boldsymbol{u}^2, \cdots, \boldsymbol{u}^M)^T$, the Eqs. (4.24) transform into

$$e^{\boldsymbol{u}^{l,n+1}} - \boldsymbol{c}^{l,n} + \gamma_l\Delta t\mathcal{A}_{\boldsymbol{c}^{l,n}}\left[q^l\boldsymbol{\psi}(\boldsymbol{u})^{n+1} + \log v_l e^{\boldsymbol{u}^{l,n+1}} - \frac{v_l}{v_0}\log\left(1-\sum_{r=1}^{M} v_r e^{\boldsymbol{u}^{r,n+1}}\right) + \sigma^l\mathcal{A}e^{\boldsymbol{u}^{l,n+1}}\right] = 0. \tag{4.25}$$

To solve (4.25), we apply the quasi-Newton's method and choose the approximated Hessian matrix as

$$\mathcal{D}_l = \big(\mathcal{I} + \gamma_l\sigma^l\Delta t\mathcal{A}_{\boldsymbol{c}^{l,n}}\mathcal{A}\big)\mathrm{diag}[e^{\boldsymbol{u}^l}] + \gamma_l\Delta t\mathcal{A}_{\boldsymbol{c}^{l,n}},$$

where $\mathcal{I}$ is an identity matrix.

In the quasi-Newton's iteration, given the previous iteration step $\boldsymbol{u}^{l,k}$, we update the concentration via

$$\boldsymbol{u}^{l,k+1} = \boldsymbol{u}^{l,k} - \eta\mathcal{D}_{l,k}^{-1}g(\boldsymbol{u}^{l,k}), \tag{4.26}$$

where

$$\begin{aligned} g(\boldsymbol{u}^{l,k}) &= e^{\boldsymbol{u}^{l,k}} - \boldsymbol{c}^{l,n} + \gamma_l\Delta t\mathcal{A}_{\boldsymbol{c}^{l,n}}\boldsymbol{\mu}_l^k, \\ \boldsymbol{\mu}_l^k &= q^l\boldsymbol{\psi}(\boldsymbol{u}^k) + \log\left(v_l e^{\boldsymbol{u}^{l,k}}\right) - \frac{v_l}{v_0}\log\left(1-\sum_{r=1}^{M} v_r e^{\boldsymbol{u}^{r,k}}\right) + \sigma^l\mathcal{A}e^{\boldsymbol{u}^{l,k}}, \end{aligned} \tag{4.27}$$

and η is the step size of the quasi-Newton's method.

To avoid the ill-conditionedness of $\mathcal{D}_{l,k}$, which was caused by the drastic change of $\boldsymbol{u}^{l,k}$, we apply the following preconditioner $\mathcal{S}_{l,k} = \mathrm{diag}[e^{-\boldsymbol{u}^{l,k}}]$, and (4.26) becomes

$$\boldsymbol{u}^{l,k+1} = \boldsymbol{u}^{l,k} - \eta(\mathcal{S}_{l,k}\mathcal{D}_{l,k})^{-1}\big[\mathcal{S}_{l,k}g(\boldsymbol{u}^{l,k})\big].$$

We have the following algorithm.

Algorithm 4.1 The quasi-Newton's method for solving JKO-1 scheme.

1: Given initial concentrations $\boldsymbol{c}^{l,0}$, obtain $\boldsymbol{\psi}^0$ by solving the Poisson's equation in matrix form (4.7).
2: Given $\boldsymbol{c}^{l,n}$ and $\boldsymbol{\psi}^n$ at time step t_n. Let $k=0$, and $\boldsymbol{u}^{l,k} = \log \boldsymbol{c}^{l,n}$.
3: Compute $\mathcal{S}_{l,k}$, $\mathcal{D}_{l,k}$, and $g(\boldsymbol{u}^{l,k})$.
4: Find $\delta\boldsymbol{u}^{l,k}$ by solving $\delta\boldsymbol{u}^{l,k} = -\eta(\mathcal{S}_{l,k}\mathcal{D}_{l,k})^{-1}[\mathcal{S}_{l,k}g(\boldsymbol{u}^{l,k})]$.
5: Update $\boldsymbol{u}^{l,k+1} = \boldsymbol{u}^{l,k} + \delta\boldsymbol{u}^{l,k}$.

6: If $\|\delta \boldsymbol{u}^{l,k}\|_\infty <$ Tol, compute $\boldsymbol{c}^{l,n+1} = e^{\boldsymbol{u}^{l,k+1}}$, $\boldsymbol{\psi}^{n+1}$ can be obtained by the Poisson's equation (4.7), and set $T = T + \Delta t$; else, $k = k + 1$, and go back to Step 3.
7: If $T \geq T_{\text{end}}$, then stop; else, let $n = n + 1$ and go back to Step 2.

Remark 4.1. In our quasi-Newton's iteration, the positivity of concentration can be preserved automatically.

5. Numerical tests

For simplicity, we consider the closed system $\Omega = [0,1] \times [0,1] nm^2$, which consists of two charged ion species K^+ and Cl^-. For simplicity, we use p and n to denote ion species K^+ and Cl^-. The solvent molecular size is $v_0 = 3.1^3 \mathring{A}^3$, and the ion sizes are $v_p = 1.51^3 \mathring{A}^3$, $v_n = 2.37^3 \mathring{A}^3$. The diffusion coefficient of p and n are $0.2\mathring{A}^2/ps$. We choose the characteristic concentration $c_0 = 1M$, the characteristic length $1nm$, the characteristic diffusion coefficient $0.2\mathring{A}^2/ps$. After dimensionless, the computational domain becomes $[0,1]^2$, and we get the nondimensionalized coefficient $\kappa = 0.19$, $\gamma_p = 0.3$, $\gamma_n = 0.3$, $v_0 = 2.0 \times 10^{-2}$, $v_p = 2 \times 10^{-3}$, $v_n = 8 \times 10^{-3}$, $\sigma^p = 0.001$, and $\sigma^n = 0.001$. Unless stated otherwise, we take the above parameters.

5.1. Accuracy

To test the accuracy of the JKO-1 scheme, we consider the following constructed problem in 2D:

$$\begin{cases} \partial_t p = \gamma_p \nabla \cdot \left(\nabla p + p \nabla \psi + \dfrac{v_p p (v_p \nabla p + v_n \nabla n)}{v_0 (1 - v_p p - v_n n)} - \sigma_p p \nabla \Delta p \right) + f_p, \\ \partial_t n = \gamma_n \nabla \cdot \left(\nabla n - n \nabla \psi + \dfrac{v_n n (v_p \nabla p + v_n \nabla n)}{v_0 (1 - v_p p - v_n n)} - \sigma_n n \nabla \Delta n) \right) + f_n, \\ -\kappa \Delta \psi = p - n + \rho^f. \end{cases} \tag{5.1}$$

The functions f_p, f_n, and ρ^f are determined by the following exact solution:

$$\begin{cases} p = 0.1 e^{-t} \cos(\pi x) \cos(\pi y) + 0.2, \\ n = 0.1 e^{-t} \cos(\pi x) \cos(\pi y) + 0.2, \\ \psi = 0.1 e^{-t} \cos(\pi x) \cos(\pi y). \end{cases} \tag{5.2}$$

The initial and boundary conditions are obtained by evaluating the exact solution at $t = 0$ and the boundary of a computational box, respectively.

We test the numerical accuracy of the proposed numerical method utilizing different spatial step size h with a fixed mesh ratio $\Delta t = h^2$. Table 1 records l^∞ errors and convergence orders for ionic concentration and electrostatic potential at time $T = 0.01$. We observe that the error decreases as the mesh refines and that the convergence orders

Table 1: Numerical error and convergence order of p, n, and ψ calculating from first-order JKO scheme (4.10) at time $T = 0.01$ with the time step size $\Delta t = h^2$ and the iteration step size $\eta = 1$.

h	l^∞ error in p	Order	l^∞ error in n	Order	l^∞ error in ψ	Order
$\frac{1}{20}$	$5.25e$-05	-	$6.82e$-05	-	$2.96e$-04	-
$\frac{1}{30}$	$2.44e$-05	1.89	$3.18e$-05	1.88	$1.33e$-04	1.97
$\frac{1}{40}$	$1.39e$-05	1.95	$1.82e$-05	1.94	$7.52e$-05	1.98
$\frac{1}{50}$	$8.98e$-06	1.97	$1.17e$-05	1.96	$4.83e$-05	1.99
$\frac{1}{60}$	$6.26e$-06	1.98	$8.18e$-06	1.98	$3.36e$-05	1.99

for ion concentrations and the potential are both about 2. This indicates that the first order scheme (4.10), as expected, is first-order and second-order accurate in time and spatial discretization, respectively. Note that the mesh ratio chosen here is for the numerical accuracy test, not for stability or positivity.

5.2. Properties test

In this case, we verify the effectiveness in preserving mass conservation, energy dissipation, and positivity of the JKO-1 scheme. We take the same parameters as the previous example, except that $\kappa = 1e$-2. Setting the initial and boundary conditions as follows:

$$\begin{cases} \psi(t,0,y) = 0.1, \;\; \psi(t,1,y) = -0.1, & y \in [0,1], \\ \dfrac{\partial \psi}{\partial y}(t,x,0) = 0.1\sin(\pi x), \;\; \dfrac{\partial \psi}{\partial y}(t,x,1) = -0.1\sin(\pi x), & x \in [0,1], \\ p(0,x,y) = 0.1, \;\; n(0,x,y) = 0.1, & (x,y) \in [0,1]\times[0,1], \\ \left(\nabla p + p\nabla\psi + \dfrac{v_p p(v_p\nabla p + v_n \nabla n)}{v_0(1 - v_p p - v_n n)} - \sigma^p p \nabla \Delta p\right)\cdot \mathbf{n} = 0 \quad \text{on } \partial\Omega, \\ \left(\nabla n - n\nabla\psi + \dfrac{v_n n(v_p\nabla p + v_n \nabla n)}{v_0(1 - v_p p - v_n n)} - \sigma^n n \nabla \Delta n\right)\cdot \mathbf{n} = 0 \quad \text{on } \partial\Omega, \\ \nabla p \cdot \mathbf{n} = 0, \;\; \nabla n \cdot \mathbf{n} = 0 \quad \text{on } \partial\Omega. \end{cases} \tag{5.3}$$

The fixed charge density is

$$\begin{aligned} \rho^f(x,y) = &-5e^{-100[(x-\frac{1}{4})^2+(y-\frac{1}{4})^2]} + 5e^{-100[(x-\frac{1}{4})^2+(y-\frac{3}{4})^2]} \\ &+ 5e^{-100[(x-\frac{3}{4})^2+(y-\frac{1}{4})^2]} - 5e^{-100[(x-\frac{3}{4})^2+(y-\frac{3}{4})^2]}. \end{aligned}$$

as is shown in Fig. 1. Here, the fixed charge density $\rho^f(x,y)$ approximates ten positive and ten negative point charges located in four quadrants using Gaussian functions with small local supports.

The prescribed potential boundary conditions represent that a potential difference is applied horizontally and the upper and lower boundaries carry surface charges with

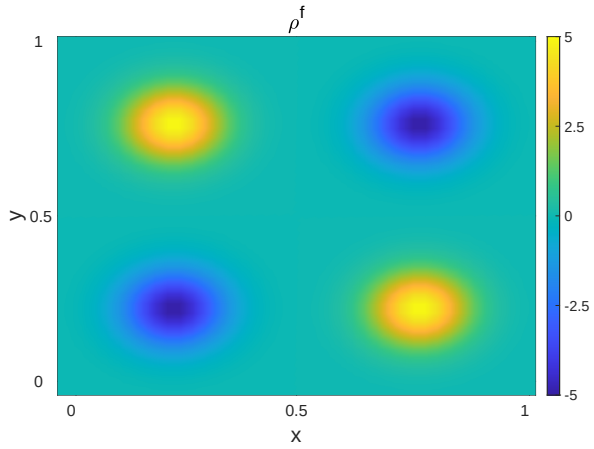

Figure 1: The distribution of fixed charge density $\rho^f(x, y)$.

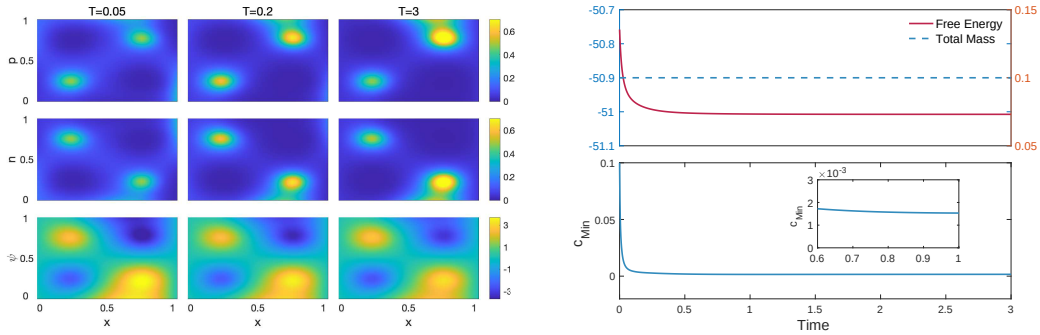

Figure 2: Left: Evolution of concentrations p, n and electrostatic potential ψ at time $T = 0.05, T = 0.2$ and $T = 3$. Right: Evolution of the discrete energy F_h, the mass of cations, and the minimum concentration with $h = 1/40$ and $\Delta t = h/10$ as time grows.

opposite signs. With such zero-flux boundary conditions and time-independent boundary potentials, the system has properties of mass conservation, free-energy dissipation.

From the left panel of Fig. 2, the concentrations p, n and the potential ψ evolves at time $T = 0.05, T = 0.2$ and $T = 3$. As time evolves, the mobile ions accumulate at the oppositely charged surfaces and fixed charges, due to electrostatic attraction. Therefore, the electrostatic potential gets screened quickly by the mobile ions of opposite signs. At time $T = 3$, the system reaches equilibrium. In the right panel of Fig. 2, as time evolves, the free energy (4.9) monotonically decreases and total conservation maintain constant. In addition, define

$$c_{\min} := \min\left\{\min_{i,j} p_{i,j}, \min_{i,j} n_{i,j}\right\},$$

which is the minimum concentrations p and n. Accordingly, the evolution of $c_{\min}$ and the zoomed-in plot verify the concentration remains positive all the time. Such results are consistent with the theoretical analysis.

5.3. Applications

In this case, we reduce our computational domain into $\Omega = [-1, 1]$ which consists of symmetric monovalent ions p and n, and take the following nondimensionalized parameters: $\kappa = 0.002, \gamma_p = 0.1, \gamma_n = 0.1, v_0 = 0.1, v_p = 0.1, v_n = 0.1, \sigma^p = 0.001$, and $\sigma^n = 0.001$. Meanwhile, considering the same boundary and initial conditions as in (5.3) except the boundary conditions for ψ which is $\psi(t, -1) = 10, \psi(t, 1) = -10$, we can get the following two graphs.

As displayed in Fig. 3, counterions are attracted to the surface due to the electrostatic interaction. Unlike the classical PNP system which predicts an unreasonable high concentration at the surface. In contrast, the counterion concentration calculated by our model is much lower, as the size effect hinders counterions from accumulating at the surface. When the charging process reaches a steady state, the counterion concentration absorbed near the surface is close to its saturation concentration $p_{\max} = 1/v_p = 10$. The same result can be obtained in the previous work by Kilic *et al.* [19]. The right plot of Fig. 3 depicts that the profiles of electrostatic potential get screened during the charging process.

To further understand the effect of the Cahn-Hilliard mixture, we consider the distribution of counterions with different σ. We use the same parameters as previous simulations, except that σ varies from 0 to 0.015. As depicted in Fig. 4, with the increase of σ, the rate of concentration p reaching the steady-state slows down. Furthermore, the concentration p will eventually reach the same saturation concentration mentioned above with different σ. This demonstrates the Cahn-Hilliard term in the SPNPCH model does not affect the saturation concentration caused by the steric effect, and only hinders the rate of reaching the steady state.

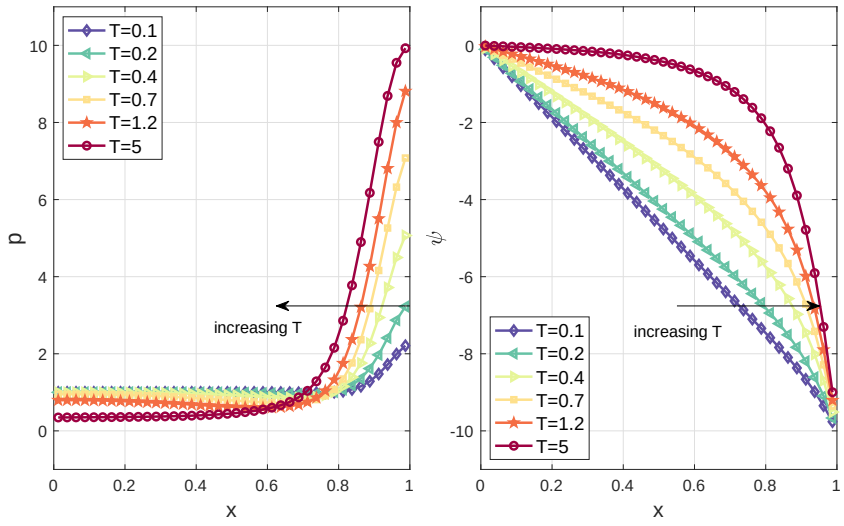

Figure 3: The concentration p (left) and the electrostatic potential ψ (right) for different time near $x = 1$.

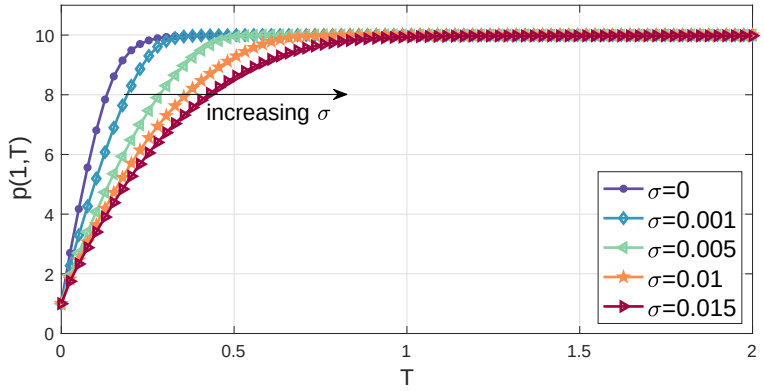

Figure 4: Concentrations p at the surface with different σ.

6. Conclusions

Due to the success of the PNP-type equations in simulating ionic concentration in semiconductors, ion channels, and electrochemical devices, structure-preserving numerical methods for constructing PNP-type equations have been popular. In this work, we propose structure-preserving numerical methods for the SPNPCH equations derived from the free energy including the electrostatic energy, the ideal-gas entropy, the steric energy, and the Cahn–Hilliard mixtures. By following the JKO technique, the SPNPCH equations can be transformed into a constrained optimization problem. Mass conservation and energy dissipation can be preserved by this scheme. In our approach, we manage to make use of the entropy terms to prevent the concentration from zero. Numerical experiments can validate the proposed scheme is first-order accuracy in time and second-order accuracy in space. Desired physical properties have been verified as well. Finally, the proposed scheme can be applied to explore the influence of ionic sizes and gradient energy coefficients on ionic distribution.

In the future, we will continue to investigate the structure-preserving JKO scheme to solve modified PNP equations including density functional theory, Coulomb ionic correlations. In addition, extending the structure grids of the proposed scheme to the nonstructural grids or irregular computational domains is of practical interest. Furthermore, one may desire that the numerical scheme of the PNP equations can keep the second-order accuracy both in time and in space. Subsequently, we will continue to consider how to construct second-order numerical schemes for PNP-type equations that preserve the structure.

Appendix A. The convex of objective function E_h^n

For any $u = (u^1, u^2, \cdots, u^M)^T$, $v = (v^1, v^2, \cdots, v^M)^T \in \mathbb{K}_{h,\delta}^M$ and $\lambda \in (0,1)$, $c(\lambda) = \lambda u + (1-\lambda)v$ is a convex, linear combination of u and v. Let ψ^1 and ψ^2 be calculated

from the Poisson's equation, corresponding to u and v. Then, $\psi(\lambda)=\lambda\psi^1+(1-\lambda)\psi^2$ is the solution to the Poisson's equation corresponding to $c(\lambda)$. We can prove that E_h^n is convex by calculating

$$E_h^n\big(c(\lambda)\big)-\lambda E_h^n(u)-(1-\lambda)E_h^n(v)=I_1+I_2+I_3+I_4\le 0,$$

where

$$\begin{aligned}
I_1=&\frac{1}{2}\left\langle\sum_{l=1}^{M}q^lc^l(\lambda)+\rho^f,\psi(\lambda)\right\rangle+\frac{1}{2}\big\langle\sigma,\psi(\lambda)\big\rangle_N-\frac{1}{2}\big\langle\psi_D,\kappa D_x\psi(\lambda)\big\rangle_D\\
&-\lambda\left(\frac{1}{2}\left\langle\sum_{l=1}^{M}q^lu^l+\rho^f,\psi^1\right\rangle+\frac{1}{2}\left\langle\sigma,\psi^1\right\rangle_N-\frac{1}{2}\left\langle\psi_D,\kappa D_x\psi^1\right\rangle_D\right)\\
&-(1-\lambda)\left(\frac{1}{2}\left\langle\sum_{l=1}^{M}q^lv^l+\rho^f,\psi^2\right\rangle+\frac{1}{2}\left\langle\sigma,\psi^2\right\rangle_N-\frac{1}{2}\left\langle\psi_D,\kappa D_x\psi^2\right\rangle_D\right)\\
=&\frac{\kappa}{2}\|\nabla_h\psi(\lambda)\|^2-\big\langle\psi_D,\kappa D_x\psi(\lambda)\big\rangle_D-\lambda\left(\frac{\kappa}{2}\|\nabla_h\psi^1\|^2-\big\langle\psi_D,\kappa D_x\psi^1{}_D\big\rangle\right)\\
&-(1-\lambda)\left(\frac{\kappa}{2}\|\nabla_h\psi^2\|^2-\big\langle\psi_D,\kappa D_x\psi^2\big\rangle_D\right)\\
\le&\frac{\kappa}{2}\Big[\big(\lambda\|\nabla_h\psi^1\|+(1-\lambda)\|\nabla_h\psi^2\|\big)^2-\lambda\|\nabla_h\psi^1\|^2-(1-\lambda)\|\nabla_h\psi^2\|^2\Big]\\
&-\kappa\big\langle D_x\psi(\lambda)-\lambda D_x\psi^1-(1-\lambda)D_x\psi^2,\psi_D\big\rangle_D\\
=&\frac{\kappa\lambda(\lambda-1)}{2}\big(\|\nabla_h\psi^1\|-\|\nabla_h\psi^2\|\big)^2\le 0,
\end{aligned}\tag{A.1a}$$

$$\begin{aligned}
I_2=&\sum_{l=1}^{M}\Big(\big\langle c^l(\lambda),\log a_l^3c^l(\lambda)-1\big\rangle-\lambda\big\langle u^l,\log a_l^3u^l-1\big\rangle-(1-\lambda)\big\langle v^l,\log a_l^3v^l-1\big\rangle\Big)\\
=&\sum_{l=1}^{M}\lambda\big\langle u^l,\log a_l^3c^l(\lambda)-\log a_l^3u^l\big\rangle+(1-\lambda)\big\langle v^l,\log a_l^3c^l(\lambda)-\log a_l^3v^l\big\rangle\\
=&-\sum_{l=1}^{M}\left[\lambda(1-\lambda)^2\left\langle\frac{u^l}{2\xi_l^2},(u^l-v^l)^2\right\rangle+\lambda^2(1-\lambda)\left\langle\frac{v^l}{2\eta_l^2},(u^l-v^l)^2\right\rangle\right]\le 0,
\end{aligned}\tag{A.1b}$$

$$\begin{aligned}
I_3=&\frac{1}{a_0^3}\left\langle\left(1-\sum_{l=1}^{M}a_l^3c^l(\lambda)\right),\log\left(1-\sum_{l=1}^{M}a_l^3c^l(\lambda)\right)-1\right\rangle\\
&-\lambda\frac{1}{a_0^3}\left\langle\left(1-\sum_{l=1}^{M}a_l^3u^l\right),\log\left(1-\sum_{l=1}^{M}a_l^3u^l\right)-1\right\rangle\\
&-(1-\lambda)\frac{1}{a_0^3}\left\langle\left(1-\sum_{l=1}^{M}a_l^3v^l\right),\log\left(1-\sum_{l=1}^{M}a_l^3v^l\right)-1\right\rangle\\
=&\lambda\left\langle\left(1-\sum_{l=1}^{M}a_l^3u^l\right),\log\left(1-\sum_{l=1}^{M}a_l^3c^l(\lambda)\right)-\log\left(1-\sum_{l=1}^{M}a_l^3u^l\right)\right\rangle
\end{aligned}$$

$$+(1-\lambda)\left\langle\left(1-\sum_{l=1}^{M}a_l^3v^l\right),\log\left(1-\sum_{l=1}^{M}a_l^3c^l(\lambda)\right)-\log\left(1-\sum_{l=1}^{M}a_l^3v^l\right)\right\rangle$$

$$=-\lambda\left\langle\left(1-\sum_{l=1}^{M}a_l^3u^l\right),\frac{1}{2\omega_l^2}\left(\sum_{l=1}^{M}a_l^3\left[u^l-c^l(\lambda)\right]\right)^2\right\rangle$$

$$-(1-\lambda)\left\langle\left(1-\sum_{l=1}^{M}a_l^3v^l\right),\frac{1}{2\nu_l^2}\left(\sum_{l=1}^{M}a_l^3\left[v^l-c^l(\lambda)\right]\right)^2\right\rangle\le 0, \tag{A.1c}$$

$$I_4=\sum_{l=1}^{M}\frac{\sigma^l}{2}\left(\|\nabla_h c^l(\lambda)\|^2-\lambda\|\nabla_h u_l\|^2-(1-\lambda)\|\nabla_h v_l\|^2\right)$$

$$\le\sum_{l=1}^{M}\frac{\sigma^l\lambda(\lambda-1)}{2}\left(\|\nabla_h u_l\|-\|\nabla_h v_l\|\right)^2\le 0. \tag{A.1d}$$

The Taylor's expansion is used in the second equality of I_2 and in the third equality of I_3. Here, ξ_l is between u_l and $c^l(\lambda)$, η_l is between v_l and $c^l(\lambda)$, ω_l is between $1-\sum_{l=1}^{M}a_l^3u_l$ and $1-\sum_{l=1}^{M}a_l^3c^l(\lambda)$, ν_l is between $1-\sum_{l=1}^{M}a_l^3v_l$ and $1-\sum_{l=1}^{M}a_l^3c^l(\lambda)$.

If only if $v=u$, the equality holds. Hence, the E_h^n is strictly convex on $\mathbb{K}_{h,\delta}^M$.

Acknowledgment

J. Ding was supported by the Natural Science Foundation of Jiangsu Province (Grant BK20210443), by the National Natural Science Foundation of China (Grant 12101264), and by the Shuangchuang program of Jiangsu Province (Grant 1142024031211190).

References

[1] L. Ambrosio, N. Gigli, and G. Savaré, *Gradient Flows: In Metric Spaces and in the Space of Probability Measures*, Springer Science & Business Media, 2005.

[2] I. Borukhov, D. Andelman, and H. Orland, *Steric effects in electrolytes: A modified Poisson-Boltzmann equation*, Phys. Rev. Lett. 79 (1997), 435–438.

[3] J. W. Cahn and J. E. Hilliard, *Free energy of a nonuniform system. I. Interfacial free energy*, J. Chem. Phys. 28(2) (1958), 258–267.

[4] C. Cancès, T. Gallouët, and G. Todeschi, *A variational finite volume scheme for Wasserstein gradient flows*, Numer. Math. 146(3) (2020), 437–480.

[5] W. Chen, C. Wang, X. Wang, and S. M. Wise, *Positivity-preserving, energy stable numerical schemes for the Cahn-Hilliard equation with logarithmic potential*, J. Comput. Phys. X, 3 (2019), 100031.

[6] J. Ding, C. Wang, and S. Zhou, *Optimal rate convergence analysis of a second order numerical scheme for the Poisson-Nernst-Planck system*, Numer. Math. Theor. Methods Appl. 12 (2019), 607–626.

[7] J. Ding, Z. Wang, and S. Zhou, *Positivity preserving finite difference methods for Poisson-Nernst-Planck equations with steric interactions: Application to slit-shaped nanopore conductance*, J. Comput. Phys. 397 (2019), 108864.

[8] J. DING, Z. WANG, AND S. ZHOU, *Structure-preserving and efficient numerical methods for ion transport*, J. Comput. Phys. 418 (2020), 109597.
[9] R. EISENBERG, Y. HYON, AND C. LIU, *Energy variational analysis of ions in water and channels: Field theory for primitive models of complex ionic fluids*, J. Chem. Phys. 133 (2010), 104104.
[10] N. GAVISH, D. ELAD, AND A. YOCHELIS, *From solvent-free to dilute electrolytes: Essential components for a continuum theory*, J. Phys. Chem. Lett. 91 (2018), 36–42.
[11] N. GAVISH AND A. YOCHELIS, *Theory of phase separation and polarization for pure ionic liquids*, J. Phys. Chem. Lett. 7(7) (2016), 1121–1126.
[12] D. GILLESPIE, W. NONNER, AND R. S. EISENBERG, *Coupling Poisson-Nernst-Planck and density functional theory to calculate ion flux*, J. Phys. Condens. Matter. 14(46) (2002), 12129.
[13] D. GILLESPIE, W. NONNER, AND R. S. EISENBERG, *Density functional theory of charged, hard-sphere fluids*, Phys. Rev. E. 68(3) (2003), 031503.
[14] T. HORNG, T. LIN, C. LIU, AND R. EISENBERG, *PNP equations with steric effects: A model of ion flow through channels*, J. Phys. Chem. B. 116(37) (2012), 11422–11441.
[15] J. HU AND X. HUANG, *A fully discrete positivity-preserving and energy-dissipative finite difference scheme for Poisson-Nernst-Planck equations*, Numer. Math. 145 (2020), 77–115.
[16] Y. HYON, B. EISENBERG, AND C. LIU, *A mathematical model for the hard sphere repulsion in ionic solutions*, Commun. Math. Sci. 9 (2010), 459–475.
[17] X. JI AND S. ZHOU, *Variational approach to concentration dependent dielectrics with the Bruggeman model*, Commun. Math. Sci. 17(7) (2019), 1949–1974.
[18] R. JORDAN, D. KINDERLEHRER, AND F. OTTO, *The variational formulation of the Fokker-Planck equation*, SIAM J. Math. Anal. 29(1) (1998), 1–17.
[19] M. KILIC, M. BAZANT, AND A. AJDARI, *Steric effects in the dynamics of electrolytes at large applied voltages. II. Modified Poisson-Nernst-Planck equations*, Phys. Rev. E. 75 (2007), 021503.
[20] D. KINDERLEHRER, L. MONSAINGEON, AND X. XU, *A Wasserstein gradient flow approach to Poisson-Nernst-Planck equations*, ESAIM Control Optim. Calc. Var. 23(1) (2017), 137–164.
[21] B. LI, *Continuum electrostatics for ionic solutions with nonuniform ionic sizes*, Nonlinearity. 22 (2009), 811–833.
[22] W. LI, J. LU, AND L. WANG, *Fisher information regularization schemes for Wasserstein gradient flows*, J. Comput. Phys. 416 (2020), 109449.
[23] T. LIN AND B. EISENBERG, *A new approach to the Lennard-Jones potential and a new model: PNP-steric equations*, Commun. Math. Sci. 12 (2014), 149–173.
[24] C. LIU, C. WANG, S. WISE, X. YUE, AND S. ZHOU, *A positivity-preserving, energy stable and convergent numerical scheme for the Poisson-Nernst-Planck system*, Math. Comput. 90(331) (2021), 2071–2106.
[25] C. LIU, C. WANG, S. M. WISE, X. YUE, AND S. ZHOU, *A second order accurate numerical method for the Poisson-Nernst-Planck system in the energetic variational formulation*, Submitted, 2021.
[26] H. LIU AND W. MAIMAITIYIMING, *Efficient, positive, and energy stable schemes for multi-D Poisson-Nernst-Planck systems*, J. Sci. Comput. 87(3) (2021), 1–36.
[27] H. LIU AND Z. WANG, *A free energy satisfying finite difference method for Poisson-Nernst-Planck equations*, J. Comput. Phys. 268 (2014), 363–376.
[28] H. LIU AND Z. WANG, *A free energy satisfying discontinuous Galerkin method for one-*

dimensional Poisson-Nernst-Planck systems, J. Comput. Phys. 328 (2017), 413–437.

[29] X. LIU, Y. QIAO, AND B. LU, *Analysis of the mean field free energy functional of electrolyte solution with non-homogenous boundary conditions and the generalized PB/PNP equations with inhomogeneous dielectric permittivity*, SIAM J. Appl. Math. 78 (2018), 1131–1154.

[30] B. LU AND Y. ZHOU, *Poisson-Nernst-Planck equations for simulating biomolecular diffusion-reaction processes I: Size effects on ionic distributions and diffusion-reaction rates*, Biophys. J. 100 (2011), 2475–2485.

[31] M. METTI, J. XU, AND C. LIU, *Energetically stable discretizations for charge transport and electrokinetic models*, J. Comput. Phys. 306 (2016), 1–18.

[32] F. OTTO, *The geometry of dissipative evolution equations: The porous medium equation*, Commun. Partial. Differ. Equ. 26 (2001), 101–174.

[33] R. PEYRE, *Comparison between W2 distance and H-1 norm, and localization of Wasserstein distance*, ESAIM Control Optim. Calc. Var. 24 (2018), 1489–1501.

[34] Y. QIAN, C. WANG, AND S. ZHOU, *A positive and energy stable numerical scheme for the Poisson-Nernst-Planck-Cahn-Hilliard equations with steric interactions*, J. Comput. Phys. 426 (2021), 109908.

[35] Y. QIAO, B. TU, AND B. LU, *Ionic size effects to molecular solvation energy and to ion current across a channel resulted from the nonuniform size-modified PNP equations*, J. Chem. Phys. 140 (2014), 174102.

[36] Y. ROSENFELD, M. SCHMIDT, H. LÖWEN, AND P. TARAZONA, *Fundamental-measure free-energy density functional for hard spheres: Dimensional crossover and freezing*, Phys. Rev. E. 55(4) (1997), 4245.

[37] J. SHEN AND J. XU, *Unconditionally positivity preserving and energy dissipative schemes for Poisson-Nernst-Planck equations*, Numer. Math. 148 (2021), 671–697.

[38] F. SIDDIQUA, Z. WANG, AND S. ZHOU, *A modified Poisson-Nernst-Planck model with excluded volume effect: Theory and numerical implementation*, Commun. Math. Sci. 16(1) (2018), 251–271.

[39] J. SLOTBOOM, *Computer-aided two-dimensional analysis of bipolar transistors*, IEEE Trans. Electron Devices. 20(8) (1973), 669–679.

[40] C. VILLANI, *Topics in Optimal Transportation*, AMS, 58, 2003.

[41] Q. ZHANG, B. TU, Q. FANG, AND B. LU, *A structure-preserving finite element discretization for the time-dependent Nernst-Planck equation*, J. Appl. Math. Comput. 68 (2022), 1545-–1564.